Heated-to-Frozen Electrochemical Interphases Formation Strategy Enables Stable 4.5 V Li-metal Batteries in Ether-based Electrolyte

Yuwei Qian,[a] Qingyu Dong*[a], Ruowei Yi,[a] Wujun Zhang,[a] Xuechun Wang,[a] Haiyang Zhang,[a] Hui Shao*[a], Patrice Simon[b],Yanbin Shen*[a], Liwei Chen,[c][d]

[a] Y. Qian, Dr. Q. Dong, Dr. R. Yi, Dr. W. Zhang, X. Wang, H. Zhang, Prof. H. Shao, Prof. Y. Shen

i-Lab, CAS Center for Excellence in Nanoscience

Suzhou Institute of Nano-Tech and Nano-Bionics (SINANO), Chinese Academy of Sciences (CAS)

Suzhou 215123, China

E-mail: gydong2017@sinano.ac.cn; hshao2023@sinano.ac.cn; ybshen2017@sinano.ac.cn

[b] Patrice Simon

Université Paul Sabatier

CIRIMAT UMR CNRS 5085, 118 Route de Narbonne

31062 Toulouse, France

[c] Prof. L. Chen

School of Chemistry and Chemical Engineering, Frontiers Science Center for Transformative Molecules, Shanghai Electrochemical Energy Device Research Center (SEED) and In-situ Center for Physical Sciences

Shanghai Jiao Tong University

Shanghai 200240, China

[d] Prof. L. Chen

Future Battery Research Center

Shanghai Jiao Tong University

Shanghai 200240, China

Supporting information for this article is given via a link at the end of the document.

Abstract: Formation of stable electrochemical interphases, including solid electrolyte interphase (SEI) and cathode electrolyte interphase (CEI) is crucial for developing high performance alkali metal batteries. The stability of SEI/CEI mainly depends on their chemistry and structure. Current studies on SEI/CEI design mainly focus on regulating their chemistry by tuning electrolyte formulations. In this work, we showcase that both the chemistry and structure of SEI/CEI could be readily regulated via a temperature modulated formation strategy. Specifically, pre-charging under heated condition was used to regulate the types and kinetics of electrolyte decomposition reactions, followed by frozen at low-temperature storage to control the deposition behavior of decomposition products on the electrode interface. Studies show that high temperatures pre-charging can affect the coordination structure of Li+ and accelerate the decomposition reaction kinetics, leading to large amount of anion decomposition. The subsequent low-temperature storage rapidly reduces the solubility of decomposition products generated at high temperatures, promoting the deposition of insoluble products on both electrodes, resulting in a dense and stable SEI/CEI. The robust SEI/CEI enables stable cycling of a 4.5 V Li||NCM811 cell in a medium-concentration ether-based electrolyte,

achieving a capacity retention of 88.7% after 200 cycles at 0.5C (areal capacity 1.5 mAh cm-2). Even under practical conditions with a high NCM811 areal loading of 4.5 mAh cm-2, the battery maintained over 80% capacity retention after 130 cycles at 0.5C. This study not only offers an economical and efficient approach to enhance the cycling stability of high-voltage lithium metal batteries but, more importantly, provides new insights into strategies for controlling the formation of SEI to improve overall battery performance.

Introduction

As the demand for energy density in electric vehicles and portable electronics continues to grow, the commercial lithium-ion battery material systems are approaching their theoretical energy density limits, making it increasingly challenging to meet future energy requirements. [1, 2]Li-metal batteries (LMBs) are considered as one of the most promising systems for next-generation high-energy-density rechargeable batteries.[3, 4] By pairing with high-nickel-content lithium nickel manganese cobalt oxides (high-Ni NCM, Ni content>60%), Li||high-Ni NCM batteries have the potential to achieve an ultra-high energy density of 500 Wh/kg.[5, 6] Further increasing the cutoff voltage (>4.4 V) of Li||high-Ni NCM cell can further boost energy density.[7] However, high-voltage Li||high-Ni NCM batteries face significant challenges, with one of the most critical being cycle stability. For both the Li-metal anode and high-Ni NCM cathode, unstable electrochemical interfaces are the primary cause of poor cycle stability.[8] The Li-metal anode tends to undergo uncontrollable side reactions with the electrolyte, leading to heterogeneous solid electrolyte interphase (SEI) formation and promoting the growth of lithium dendrites, which rapidly deteriorate the life-span of LMBs.[9] While the high-Ni NCM cathode is prone to interfacial structural degradation and transition metal dissolution under high-voltage, further compromising the long-term stability of the battery.[10] The key to overcoming these challenges lies in the design and construction of stable electrochemical interfaces, including the formation of robust SEI and cathode electrolyte interphase (CEI) layers, which are crucial for enhancing the cycling performance of Li||high-Ni NCM batteries.[11]

The SEI and CEI are formed through the decomposition of electrolyte components adsorbed on the inner Helmholtz layer of the electrode surface.[12] During electrochemical cycling, the electrolyte undergoes redox reactions at the electrode surface driven by the electrochemical potential, and the resulting reaction products precipitate onto the electrode surface, forming a multicomponent passivation layer (SEI/CEI) that inhibits further electrolyte decomposition by blocking electronic conduction.[13] The composition of the SEI/CEI is influenced by various factors, including the composition of the electrolyte, the electrode material, the and so on.[7] Certainly, the same electrolyte will form different passivation layers on the anode and cathode surfaces due to the distinct electrochemical potentials at each interface. For example, while the ester-based electrolytes commonly used in lithium-ion batteries can effectively accommodate the requirements of high-voltage cathode materials, the ester solvent molecules tend to engage in persistent and uncontrolled side reactions with the highly reactive Li-metal, making it difficult to form a stable SEI, leading to low coulombic efficiency and short cycle life and severely limiting their application in LMBs.[14, 15] In contrast, ether-based electrolytes could form an uniform and stable SEI on the lithium metal surface, demonstrating better compatibility with LMBs. [16, 17] However, ether-based electrolytes suffer from poor oxidative stability, particularly under high-voltage conditions, when oxidative decomposition on the highly reactive high-Ni NCM cathode surface is exacerbated, making it challenging to apply ether-based systems to high-voltage battery systems (>4.4 V).[18, 19]

To improve the stability of high-voltage LMBs, researchers have proposed various strategies to modulate the composition of SEI/CEI by designing the electrolyte composition, including the incorporation of functional additives,[20, 21] lithium salt design,[22, 23] high-concentration electrolytes,[24, 25] localized high-concentration electrolytes,[26] and functional group design of solvent molecules.[27, 28] In addition, recent studies have also suggested that external factors such as electric fields and temperature can regulate SEI formation without altering the electrolyte composition.[29, 30] Although these strategies employ different methods to enhance the cycling stability of high-voltage LMBs, their core design philosophy remains consistent: controlling the composition of SEI/CEI by regulating the types of electrolyte decomposition reactions. Undoubtedly, the decomposition reactions of the electrolyte at the electrode surface and the resulting products are key factors influencing the stability of

SEI/CEI. However, other crucial aspect of SEI/CEI formation—namely, the deposition and recombination kinetics of electrolyte decomposition products—remains largely overlooked.

Herein, we present a simple yet effective strategy to modulate both the chemistry types and kinetics of electrolyte decomposition reactions, as well as the deposition and recombination of decomposition products, through precise control of the formation temperature. This approach enables the formation of stable SEI/CEI layers on Li metal anode/high Ni cathode, significantly enhancing the cycling stability of high-voltage Li||high-Ni NCM batteries in an ether-based electrolyte. High-temperature (HT, 60 °C) pre-charging was utilized to regulate the decomposition chemistry and kinetics, while low-temperature storage (LT, -20 °C) was applied to control the deposition of decomposition products on the electrode interface, resulting in the formation of robust and stable CEI/SEI layers. The designed interphases allowed the medium-concentration ether-based electrolyte to operate stably at voltages as high as 4.5 V. The Li||high-Ni NCM battery demonstrated a specific capacity of 179.2 mAh g^{-1} and a capacity retention of 88.7% after 200 cycles at 0.5C with an $LiNi_{0.83}Co_{0.05}Mn_{0.12}O_2$ (NCM811) electrode loading of 1.5 mAh cm^{-2}, while significantly reducing voltage polarization. Even at a practical high areal capacity of 4 mAh cm^{-2}, the capacity retention exceeded 80% after 130 cycles at 0.5C. This study not only offers a cost-effective approach to enhancing the cycling stability of high-voltage LMBs, but more importantly, it provides new insights into strategies for regulating the formation of electrochemical interphases to improve overall battery performance.

Results and Discussion

Electrolyte Solvation Structure and Decomposition Kinetics.

The SEI/CEI formation process primarily involves the initial charge-discharge cycles of the battery, during which the solvents and lithium salts in the electrolytes undergo a series of redox reactions. [31] The resulting reaction products subsequently deposit on the surfaces of the cathode and anode materials, leading to the formation of the CEI and SEI layers. Since temperature will not only affect the redox reaction kinetics but also the deposition behavior of the insoluble decomposing products, we propose a formation process that combines high-temperature pre-charging and low-temperature storage to regulate the formation of SEI and CEI. As schematically illustrated in Figure 1a, compared to formation of SEI/CEI at room temperature, high-temperature pre-charging could affect the solvation structure of lithium ions thus enabling the regulation of SEI/CEI composition, and also accelerate the decomposition kinetics of electrolyte components on the electrode surface, producing large amount of designed decomposition products for SEI/CEI formation.[32] More importantly, after the high-temperature pre-charging process, treated the batteries with low-temperature storage could cause a rapid decrease in the solubility of the electrolyte decomposition products, resulting in the formation of a dense electrochemical interfaces on both the cathode and anode. By combining high-temperature pre-charging and low-temperature storage, we aim to build stable SEI and CEI and enable long term cyclability of high-voltage Li||NCM811 cell in an ether-based electrolyte.

As a proof of concept, we employed a medium-concentration ether-based electrolyte (0.6 M LiTFSI + 0.6 M LiDFOB in DME + FEC [7:3 by weight], LLDF) in Li||high-Ni NCM battery system. First of all, we aim to maximize the involvement of anions rather than DME solvent molecules in the CEI formation reaction. Recent reports have indicated that temperature can modulate the solvation structure of lithium ions.[30, 33, 34] We also found that the solvation structures of the lithium-ions in the aforementioned ether-based electrolyte changes with temperature. Classical molecular dynamics (MD) simulations were first employed to investigate the evolution of the Li^+ solvation structure with various temperatures (Figure S1). The radial distribution functions (RDFs) are presented in Figures 1b to d. The calculated coordination number statistics at different temperatures (Figure 1e) show that the coordination capability of the lithium ion with the solvents is enhanced at elevated temperatures, leading to an increase in the number of DME and FEC molecules in the first solvation shell, while the number of anions in this shell decreases, resulting in more uncoordinated $DFOB^-$ anions in the solution. More specifically, a Li^+ ion, on average, coordinates with 2.23 DME molecules, 0.91 FEC solvents, 0.92 $TFSI^-$, and 0.27 $DFOB^-$ in its innermost solvation shell at RT (Table S1). When the temperature is elevated to 60 °C, the coordination numbers for $TFSI^-$

and $DFOB^-$ decrease to 0.9 and 0.08, respectively, while those for DME and FEC increase to 2.57 and 1.03, respectively. The enriched DME number in solvation structure could due to the small molecular size of DME, which allows it to rapidly coordinate with Li^+ in a dynamic fashion, and its relative stability at higher temperatures. Additionally, increased molecular thermal motion at elevated temperatures and the enhanced competitive coordination of DME could displace $DFOB^-$ from coordination, leading to the presence of free $DFOB^-$ anions. During charging, Li^+ migrates to the anode along with solvating solvent molecules and anions, while the non-solvated anions migrate towards the inner Helmholtz plane (IHP) on the cathode side under the influence of the electric field,[35] as depicted in Figure 1f. In the initial charging process, the relatively higher proportion of $DFOB^-$ and the reduced presence of DME within the IHP at the cathode (NCM811) could facilitate the formation of a CEI rich in inorganic components, such as LiF and boron-oxygen compounds, effectively suppressing further electrolyte decomposition during subsequent electrochemical cycles. Therefore, pre-charging at 60 °C was selected for our temperature regulation strategy, given the significant change in the solvation structure of lithium ions at this condition, rationalizing our design concept of regulating the IHP through temperature control to influence electrolyte decomposition chemistry. It is noteworthy that previous works have primarily used high-concentration electrolytes or locally high-concentration electrolytes to regulate the solvation structure of lithium ions, which often increases viscosity and cost of the electrolyte.[36] In contrast, the high-temperature pre-charging strategy proposed in this study is simple and feasible, with promising potential for large-scale application.

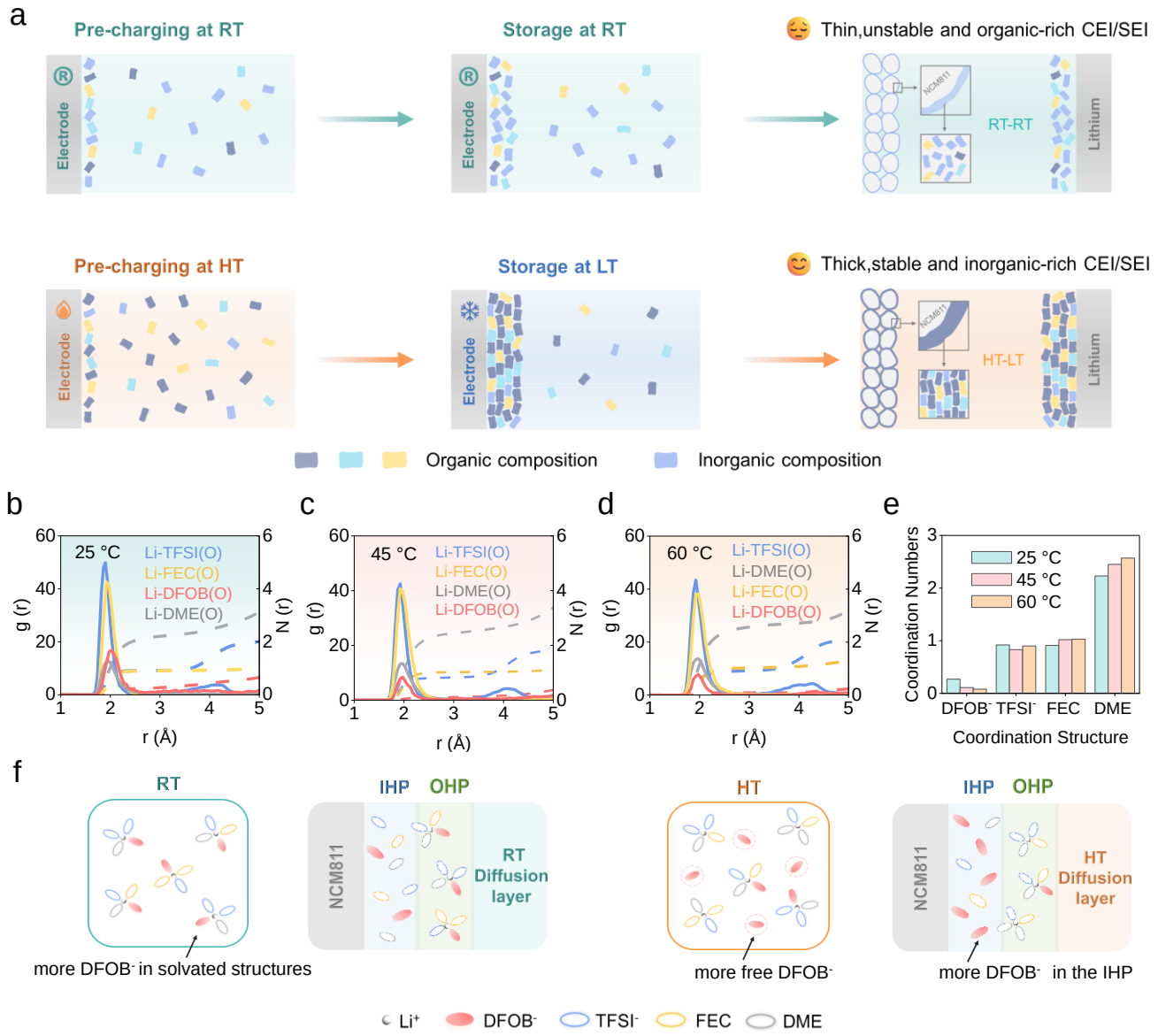

Figure 1. The design principles of temperature modulated strategy. (a) Schematic illustrations of the temperature modulated

electrochemical interphase formation process. The radial distribution functions (RDF) and coordination number (N(r)) of the LLDF electrolyte obtained from the MD simulation at (b) 25 °C, (c) 45 °C and (d) 60 °C. (e) The coordination numbers of Li^+ at various temperatures. (f) The temperature regulation influencing the solvation structure and modifying the IHP during the pre-charging process.

To further elucidate the impact of temperature on the solvation structure of lithium ions, nuclear magnetic resonance (NMR) measurements were conducted at RT and 60 °C. Figure 2a shows the ^{7}Li-NMR spectra, where an upfield shift of the ^{7}Li signal is observed with increasing temperature, indicating that the interaction between Li^+ and the solvents strengthens, leading to a more localized electron cloud density around the Li^+ ions.[37] Moreover, the appearance of a second peak besides the main peak suggests the possible emergence of different solvation structures at higher temperatures. Combining these findings with the MD results (see Note 1 in Supporting information), we speculate that this additional peak may result from a reduction in the coordination number of $DFOB^-$ anions, leading to a solvation structure within the contact ion pairs that lacks $DFOB^-$ in the Li^+ solvation shells. Fourier-transform infrared (FTIR) spectroscopy was also employed to analyze the effect of temperature on the Li^+ solvation structure, as shown in Figure 2b. Due to the Fermi resonance effect, the FEC molecule exhibits two carbonyl (C=O) absorption peaks at 1833.7 cm^{-1} and 1806.8 cm^{-1}, with the carbonyl peak at 1806.8 cm^{-1} overlapping with the carbonyl peak of $DFOB^-$.[38] As the temperature increases, the characteristic peak at 1833.7 cm^{-1} shifts to a higher wavenumber of 1835.9 cm^{-1}, indicating enhanced coordination between FEC and Li^+. Meanwhile, the other characteristic peak at 1806.8 cm^{-1} shifts significantly to a lower wavenumber of 1803.8 cm^{-1}, suggesting a weakened coordination between Li^+ and $DFOB^-$.[38] Raman spectroscopy results of the electrolyte at different temperatures are presented in Figure 2c. The characteristic peak corresponding to the bending vibration of the S-N-S group in LiTFSI shifts from 735.0 cm^{-1} at RT to 736.1 cm^{-1} at HT, indicating an enhanced interaction between Li^+ and $TFSI^-$ at elevated temperatures.[18] Meanwhile, the characteristic peak corresponding to ring-breathing mode of $DFOB^-$ redshifts from 713.4 cm^{-1} at RT to 712.7 cm^{-1} at HT, suggesting a weakened coordination ability between Li^+ and the $DFOB^-$ anion at higher temperatures.[39, 40] These FTIR and Raman observations are well aligned with the MD simulation results.

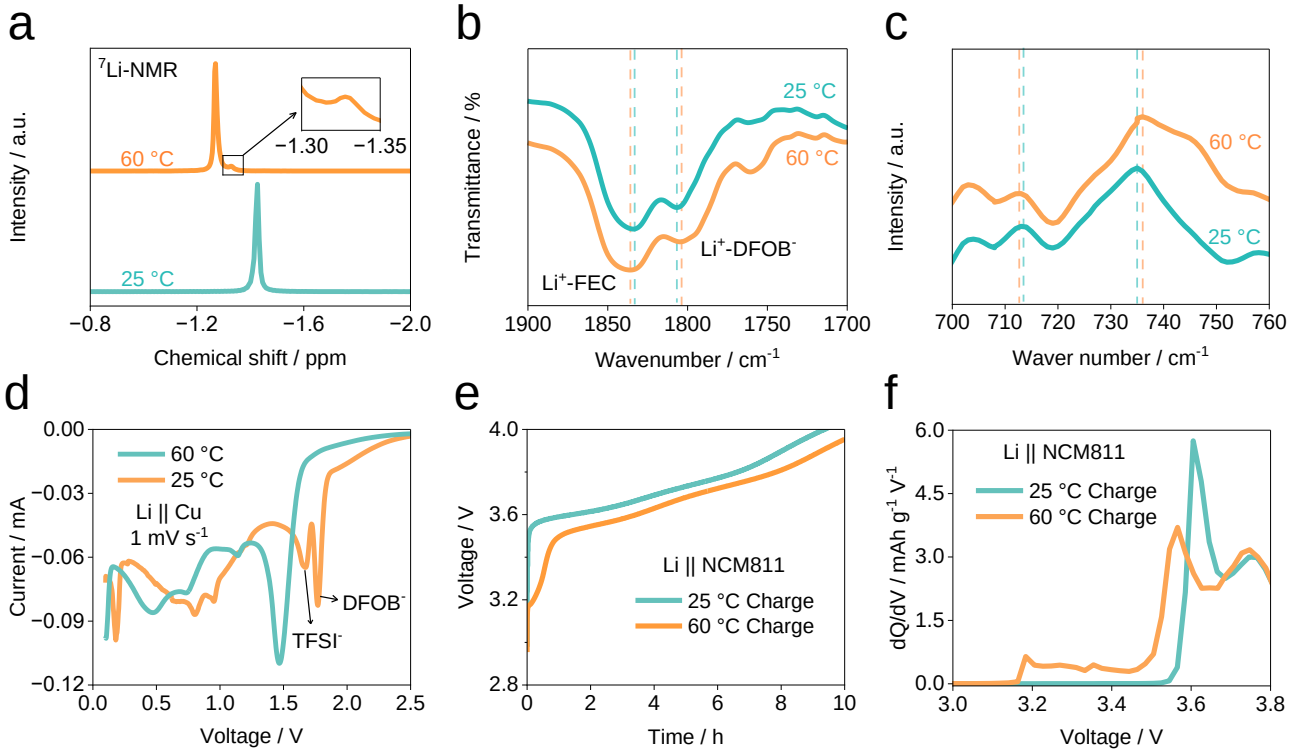

Figure 2. Temperature modulated strategy for regulating the CEI/SEI formation process. (a) ^{7}Li-NMR, (b) FT-IR and (c) Raman results of the LLDF electrolyte under different temperatures. (d) LSV curves comparing the reduction reactions of the LLDF electrolyte at the low cutoff voltage range with a cell configuration of Li||Cu. (e) The pre-charging profiles of Li||NCM811 cells and (f) corresponding differential capacity curves at different temperature.

In addition to regulating the solvation structure, high-temperature pre-charging could also effectively enhance

the decomposition kinetics of the electrolyte at both the cathode and anode sides, thereby achieving rapid electrochemical interphase layers formation. We first employed linear sweep voltammetry (LSV) to compare the effect of temperature on the reduction reaction at low potentials and the oxidation reaction at high potentials in the electrolyte. As shown in Figure 2d, the reduction peaks at 1.5 V and 1.14 V at the room temperature correspond to the decomposition of $DFOB^-$ and $TFSI^-$, respectively.[41, 42] However, due to changes in solvation structure and the intensified reduction reactions at elevated temperatures, these peaks shift to 1.77 V and 1.6 V, respectively. This shift may promote the formation of an SEI layer on the anode side, primarily composed of decomposition products from DFOB and TFSI. Moreover, the oxidation peak shifts to a lower potential as presented in Figure S2. These results suggesting that the side reactions associated with electrolyte decomposition are more pronounced at elevated temperatures. Figures 2e and f compare the constant current charge-discharge curves and corresponding differential capacity voltage curves of Li||NCM811 cells pre-charged at 0.1C at different temperatures. It is evident that significant side reactions are observed before 3.5 V at 60 °C. This further demonstrates that high temperatures exacerbate electrolyte side reactions during the initial charge, leading to the formation of more extensive electrochemical interphase compounds. After pre-charging to 4.0 V at 60 °C, the cells were subsequently stored at -20 °C for 12 hours. Since the solubility of the electrolyte decomposition products generated during the high-temperature pre-charge decreases at low temperatures, we anticipate that this frozen process would accelerate the deposition of by-products on both electrodes and is expected to result in more compact and stable SEI and CEI, which will be further elaborated in the following discussions.

Structure and Chemistry of Interphases.

To investigate the impact of temperature-regulated formation strategies on the electrochemical interphases, we conducted an in-depth analysis of the interfacial structure and composition of Li||NCM811 cells under different formation conditions: high-temperature (60 °C) pre-charging followed by low-temperature (-20 °C) storage for 12 hours (denoted as HT-LT), high-temperature (60 °C) pre-charging followed by room-temperature (25 °C) storage for 12 hours (denoted as HT-RT), and room-temperature (25 °C) pre-charging followed by room-temperature (25 °C) storage for 12 hours (denoted as RT-RT), more details can be found in Supporting information. Using high-resolution transmission electron microscopy (TEM), we first examined the CEI thickness on the NCM811 side under different formation conditions. The CEI thickness on the surface of NCM811 was approximately 2.1-3.4 nm for the RT-RT condition (Figure 3a). When the pre-charging temperature was increased, the CEI thickness in the HT-RT condition significantly increased to approximately 2.91-5.54 nm (Figure 3b). Under the high-temperature pre-charging and low-temperature storage condition, the HT-LT condition resulted in the thickest CEI, measuring approximately 6.7-7.9 nm (Figure 3c). Additionally, SEM analysis of NCM (Figure S3) showed that, compared to the smooth prstine NCM811 surface, the HT-LT NCM811 surface exhibited more flocculent decomposition products.

Further chemical composition analysis of the CEI on various NCM811 surfaces was conducted using X-ray photoelectron spectroscopy (XPS). The measured C 1s, O 1s, and F 1s spectra of the NCM811 electrodes disassembled from the RT-RT and HT-LT cell were showed at Figure S4 and the results were summarized and presented at Figure 3d-f. From the C 1s spectra (Figure 3d), we observed that under HT-LT formation conditions, the proportion of $ROCO_2Li$ organic lithium salts, which are derived from the decomposition of solvents including DME and FEC, is reduced compared to the RT-RT conditions.[43] Conversely, the proportions of lithium carbonate and fluorine-containing organic compounds ($CH\text{-}CF_2$), primarily generated from FEC decomposition, are increased.[44] The O 1s spectra (Figure 3e) further reveal a weakening of the M-O signal in the HT-LT treated electrode, indicating that the CEI becomes thicker and more uniform in the HT-LT electrode, covering more of the NCM811 cathode surface and thus reducing the exposure of transition metals, consistent with TEM observations.[45] Additionally, the significant increase in B-O content under HT-LT conditions suggests the formation of more inorganic B-O compounds within the CEI.[46] The F 1s spectra (Figure 2f) also show a marked increase in the levels of inorganic components such as LiF and B-F under HT-LT conditions. Time-of-flight secondary ion mass spectrometry (TOF-SIMS) analysis comparing the interfacial phase compositions between RT-RT and HT-LT conditions (Figures 3g, h and i) demonstrating a higher concentration of inorganic components on the HT-LT electrode surface, including $LiCO_3^-$, BO^- and LiF^-. The TOF-SIMS results further confirmed that the CEI formed

under HT-LT conditions possess more inorganic-rich components such as Li_2CO_3, LiF, and B-O compounds, which agrees well with the XPS findings.[45] The increase in inorganic components within the CEI on the cathode side can be attributed to our temperature-controlled CEI formation strategy. Specifically, as previously discussed, the higher temperature during the charging process leads to an increased presence of $DFOB^-$ in the IHP on the NCM811 surface, resulting in more $DFOB^-$ participation in CEI formation under HT-LT conditions. Moreover, the elevated temperature promotes the decomposition of $DFOB^-$ and FEC, while subsequent low-temperature storage likely accelerates the accumulation of decomposition products, leading to the formation of a denser CEI layer. Based on above discussions, we demonstrated that the HT-LT-formed CEI contains a higher proportion of inorganic components, which could effectively enhance the electrochemical stability of the interfacial phase. Furthermore, the thicker and denser CEI provides better coverage and protection of the NCM811 cathode surface, reducing the dissolution of transition metals and the side reactions with DME. These favorable factors are expected to significantly improve the electrochemical interfacial stability of NCM811 in ether-based electrolytes under high cutoff voltages, thereby enhancing its cycling performance.

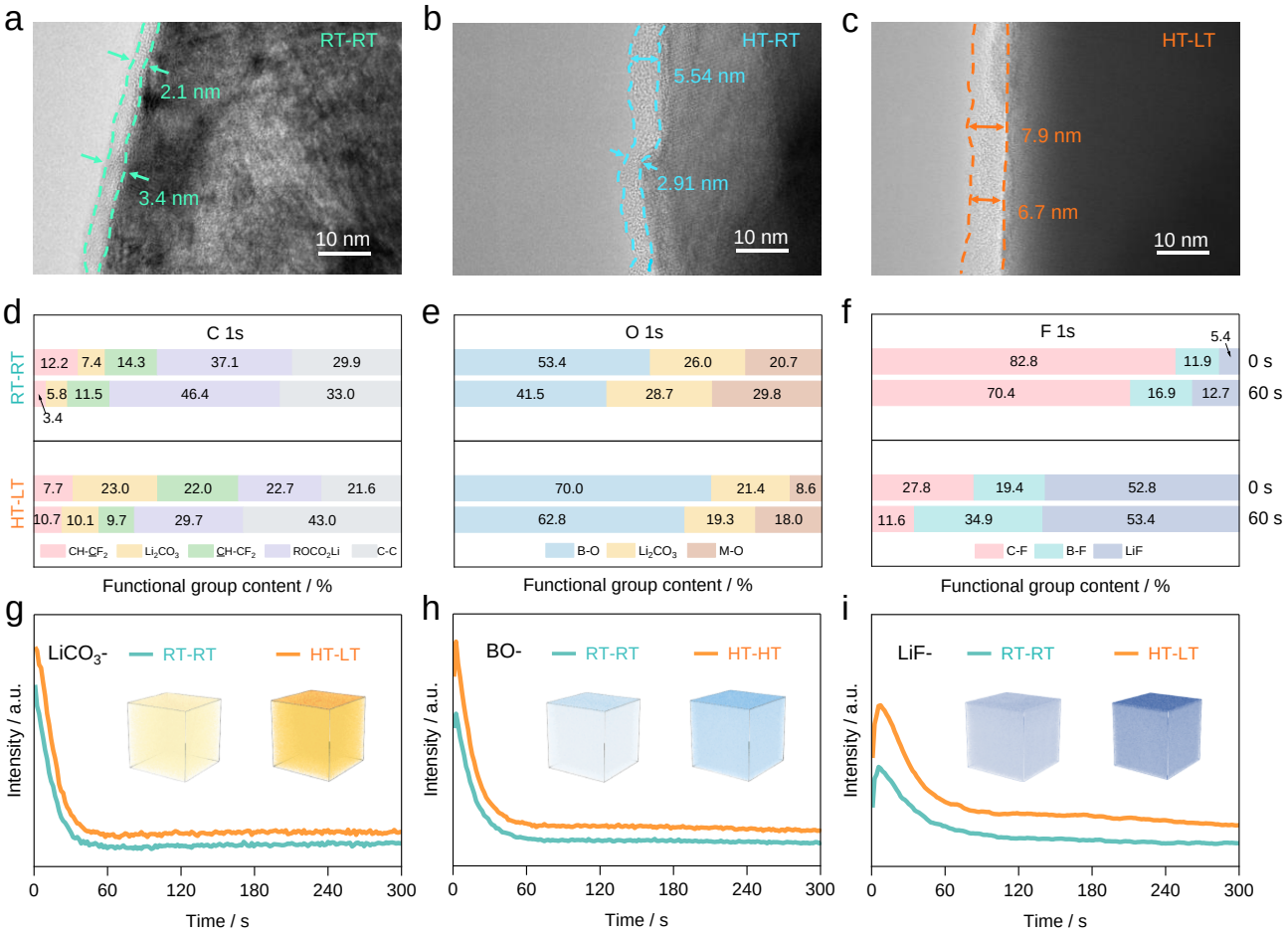

Figure 3. Characterizations of CEI on NCM811 cathode. HR-TEM showing the thickness of CEI of (a) RT-RT NCM811, (b) HT-RT NCM811, and (c) HT-LT NCM811. Surface chemical composition comparing of RT-RT NCM811and HT-LT NCM811 obtained from XPS analysis of (d) C 1s, (e) O 1s, and (f) F 1s. The in-depth TOF-SIMS profiles of (g) $LiCO_3^-$, (h) BO^-, and (i) LiF^- of RT-RT and HT-LT NCM811. Insets give the 3D ToF-SIMS mapping distribution of related compounds.

Under the HT-LT strategy, we also obtained a more beneficial SEI that enhances the stability of the Li metal anode. As discussed earlier, at elevated temperatures, more electrolyte components could participate in SEI formation on the Li metal anode, and during subsequent low-temperature storage, a thicker SEI layer could be formed. The chemical components of the SEI layers formed on the Li metal sides were first investigated using XPS techniques (Figure S5). XPS analysis of the C 1s spectrum (Figure 4a) revealed a decreased proportion of organic alkyl lithium species under HT-LT conditions. The O 1s spectrum (Figure 4b) showed a weakened M-O signal, indicating that the SEI layer becomes thicker at higher temperatures. The comparison of the F 1s spectra (Figure

4c) demonstrated an increase in the LiF content under HT-LT conditions. Furthermore, TOF-SIMS analysis indicated that the lithium metal surface under HT-LT conditions contained higher concentrations of $LiCO_3^-$, BO^-, and LiF^-. These results suggest that the SEI formed on the lithium metal under HT-LT conditions is thicker and richer in inorganic components. These inorganic compounds are beneficial for forming a stable barrier within the SEI, effectively preventing continuous reactions between Li metal and the electrolyte and reducing the occurrence of side reactions in subsequent cycles, thereby enhancing interfacial stability. Additionally, a thicker and more inorganic-rich SEI provides mechanical strength, mitigating the growth and penetration of lithium dendrites, and preventing short circuits and capacity degradation during cycling.

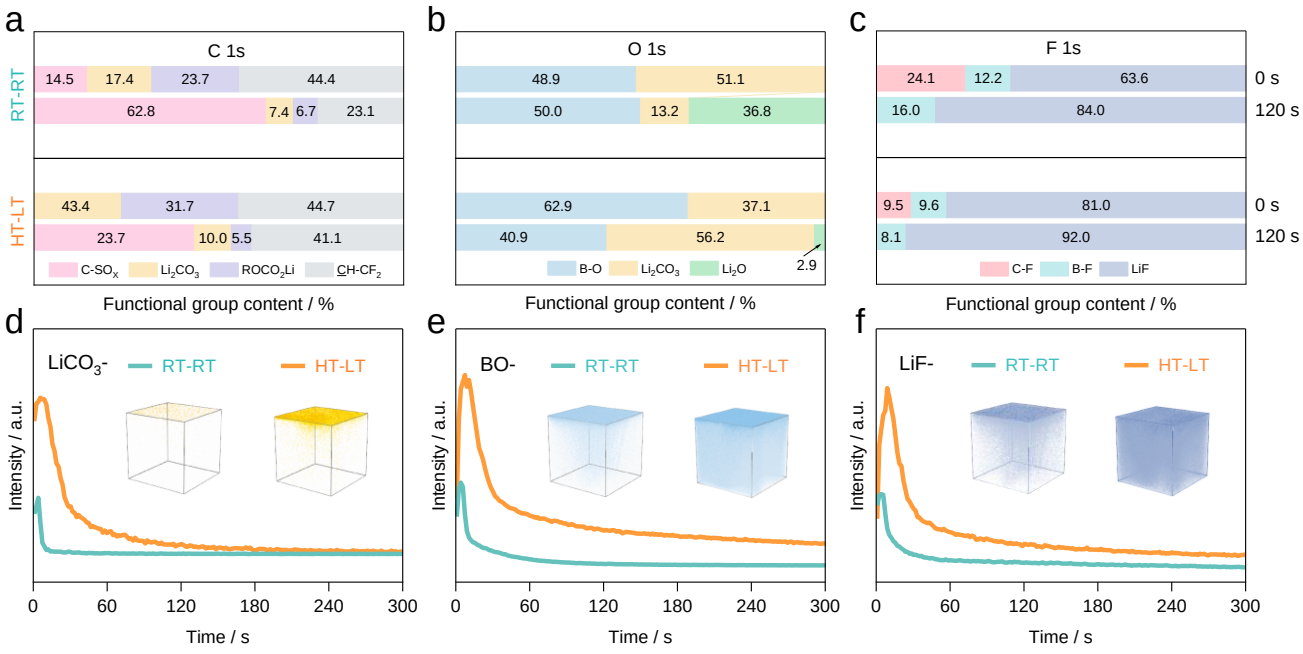

Figure 4. Characterizations of SEI on Li metal anode. Surface chemical composition comparing of RT-RT Li anode and HT-LT Li anode obtained from XPS analysis of (a) C 1s, (b) O 1s, and (c) F 1s. The in-depth TOF-SIMS profiles of (d) $LiCO_3^-$, (e) BO^-, and (f) LiF^- of RT-RT and HT-LT Li anode. Insets give the 3D TOF-SIMS mapping distribution of related compounds.

To verify the stability of the SEI/CEI formed by our temperature-regulated strategy, we first tested the cycling stability of Li||NCM811 cells with ether-based electrolytes under three different formation methods at a charge-discharge interval of 2.8-4.5V at a 0.5C rate. As shown in Figure 5a, the specific capacity of RT-RT cell rapidly dropped from 203.1 mAh g^{-1} (based on the NCM811 electrode) to 136.2 mAh g^{-1} after 200 cycles, with the capacity retention of RT-RT of 66.9%. After high-temperature pre-charging, the capacity retention of HT-RT increased to 81.0%, indicating that high-temperature pre-charging significantly improved cycling stability. Combining high-temperature pre-charging and low-temperature storage, the HT-LT Li||NCM811 cell maintained a specific capacity of 179.2 mAh g^{-1} after 200 cycles, with an enhanced capacity retention of 88.7%. In addition to improved capacity retention, the temperature-regulated measures significantly reduced voltage polarization during the cycling of Li||NCM811 (Figure 5b-c and Figure S6). We further tested the cycling stability of Li||NCM811 cells with the NCM811 electrode areal capacity reaching the practical application level of 4.5 mAh cm^{-2} (24.5 mg cm^{-2}) at the high cutoff voltage of 4.5 V. The capacity retention after 130 cycles at 0.5 C (corresponding to a high charge/ discharge current density of 2 mA cm^{-2}) was 80.2%, which is superior to the RT-RT condition. Clearly, the stable SEI/CEI formed under the temperature-regulated strategy effectively improved the cycling stability of Li||NCM811 at high voltages in ether-based electrolyte systems, including high capacity retention and reduced voltage polarization accumulation. The rate performance of HT-LT and RT-RT was also compared, and it was observed that HT-LT exhibited superior rate performance at 3C charge-discharge rates, as shown in Figure S7. We speculate that the enhanced rate performance is due to the more stable electrochemical interphase of HT-LT, while the electrochemical interphase of RT-RT continues to evolve during the initial low-rate cycles, leading to increased interfacial impedance.

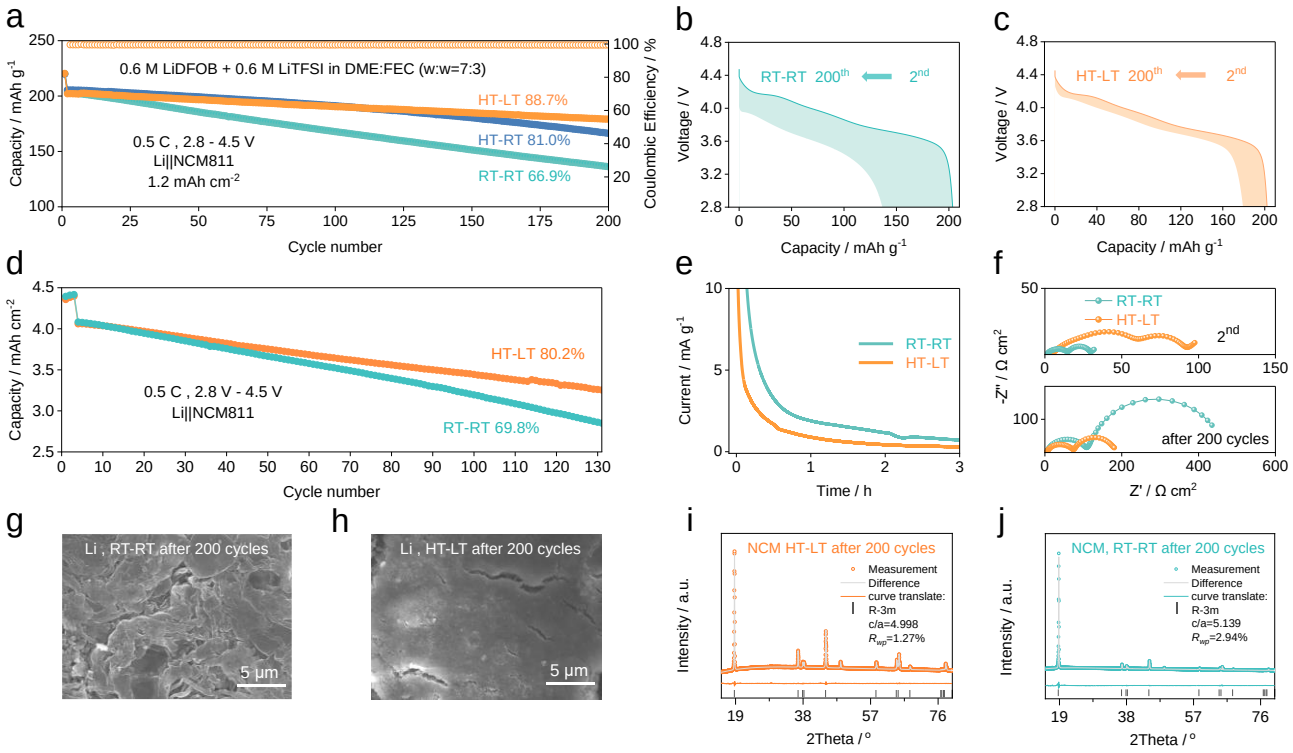

Figure 5. Electrochemical tests of Li||NCM811 cells after different formation process and characterizations of anodes and cathodes post cycling. (a) Electrochemical cycling stability of Li||NCM811 cells after different formation process. Charging profiles of electrochemical cycling test of (b) RT-RT and (c) HT-LT Li||NCM811 cells. (d) Electrochemical cycling stability of Li||NCM811 cells with higher areal capacity. (e) Rate capability of Li||NCM811 cells after different formation process. (e) CA test of RT-RT and HT-LT cells at 4.5 V after formation. (f) EIS comparison of RT-RT and HT-LT cells before and after 200 cycles. SEM images showing the surface morphology of (g) RT-RT Li anode and (h) HT-LT Li anode after 200 cycles. XRD analysis of (i) HT-LT NCM811 cathode and (j) RT-RT NCM811 cathode after 200 cycles.

CA testing was employed to further understand the stability of the SEI/CEI formed under different conditions. Compared to RT-RT, HT-LT exhibited a lower and more rapidly stabilized leakage current when held at 4.5V (Figure 5e), further indicating the formation of a denser and more stable SEI/CEI under the temperature-regulated strategy. We conducted EIS impedance measurements of Li||NCM811 before and after 200 cycles, as shown in Figure 5f. Post-cycling, the interfacial impedance of RT-RT cells increased sharply, correlating with the rapid decline in cycling performance. In contrast, the impedance change of HT-LT cells was relatively minor, indicating a more stable electrochemical interphase. Morphological examination of the lithium metal anode side revealed that after 200 cycles, the RT-RT condition (Figure 5g) exhibited a loose morphology with significant lithium dendrite growth. Conversely, the HT-LT condition (Figure 5h) showed a more compact and smooth lithium metal surface, with no apparent dendrite formation. We also analyzed the evolution of the CEI on NCM811 after cycling (Figure S8). The O 1s spectra reveal a significant decrease in the intensity of the M-O signal under RT-RT conditions after cycling, indicating an increase in CEI thickness. Furthermore, the F 1s spectra show that the C-F components in the CEI initially present on the RT-RT electrode transformed into LiF after cycling, suggesting substantial compositional changes in the CEI formed under RT-RT conditions. In contrast, the CEI obtained under HT-LT conditions exhibited insignificant changes after cycling, indicating excellent stability of the temperature regulated CEI. The thicker CEI on the cycled RT-RT NCM811 electrode was also verified by SEM analysis (Figure S9). We further conducted the XRD analysis after 200 cycles for both NCM811 electrode (Figures 5i and j). Rietveld refinement reveals that the c/a lattice parameter ratio for NCM811 electrode with RT-RT-formed CEI is 5.139, while for the HT-LT-formed CEI it is 4.998. Note that the pristine c/a lattice parameter ratio for NCM811 is 4.947 (Figure S10). A higher c/a ratio, as observed in the RT-RT NCM811 electrode, suggests greater lattice distortion, which is often associated with the degradation of the NCM811 material, such as transition metal migration and structural collapse. [45, 47] This structural instability can lead to a decline in electrochemical performance over extended cycling. In contrast, the lower c/a ratio in the HT-LT electrode indicates less lattice distortion, implying that the CEI formed in HT-LT method provides

better mechanical and chemical protection to the NCM811 crystal structure, maintaining the integrity and reducing the degradation. These results collectively demonstrate that the SEI/CEI formed through the temperature-regulated formation process is more stable, significantly enhancing the electrochemical performance of high-voltage lithium metal batteries in ether-based electrolytes.

Conclusion

In this study, we propose a straightforward and facile high-low temperature formation strategy that achieves a more stable electrochemical interphase by regulating solvation structure and reaction rates. This process significantly enhances the high-voltage (4.5 V) performance of Li||NCM811 batteries in a medium-concentration ether-based electrolyte system. By pre-charging at 60 °C and then storing at -20 °C, we obtained a highly stable electrochemical interphase on both NCM811 cathode and Li metal anode sides. As a result, the Li||NCM811 cell exhibited a specific capacity of 179.2 mAh g^{-1} and a capacity retention of 88.7% after 200 cycles at 0.5C with a NCM811 areal capacity of 1.5 mAh cm^{-2}, with significantly reduced voltage polarization. At a practical application level with a high areal capacity of 4.5 mAh cm^{-2}, the capacity retention of Li||NCM811 cell at 0.5C exceeded 80% after 130 cycles. Our proposed HT-LT formation procedure shows promising potential for the large-scale production of high-performance lithium metal batteries, offering an economical and efficient approach to achieving excellent stability and longevity in high-voltage operations. This works also offers new insights into achieving enhanced battery performance without altering the electrolyte composition.

Acknowledgements

This work was financially supported by the National Natural Science Foundation of China (Grant no.22179143 and 22309202, and the Gusu Leading Talents Program (ZXL2023190). We also acknowledge the technical support for Nano-X from Suzhou Institute of Nano-Tech and Nano-Bionics, Chinese Academy of Sciences (SINANO).

Keywords: Lithium Metal Battery, High-Voltage, SEI/CEI Formation, Temperature Modulation, Ether-Based Electrolyte

[1] He M N, Hector L J R, Dai F, et al. Industry needs for practical lithium-metal battery designs in electric vehicles[J]. Nature Energy, 2024, 9(10): 1199-1205.

[2] Yuan S Y, Kong T Y, Zhang Y Y, et al. Advanced Electrolyte Design for High-Energy-Density Li-Metal Batteries under Practical Conditions[J]. Angewandte Chemie-International Edition, 2021, 60(49): 25624-25638.

[3] Liu J, Bao Z N, Cui Y, et al. Pathways for practical high-energy long-cycling lithium metal batteries[J]. Nature Energy, 2019, 4(3): 180-186.

[4] Yu Z, Wang H S, Kong X, et al. Molecular design for electrolyte solvents enabling energy-dense and long-cycling lithium metal batteries[J]. Nature Energy, 2020, 5(7): 526-533.

[5] Kim S, Park G, Lee S J, et al. Lithium-Metal Batteries: From Fundamental Research to Industrialization[J]. Advanced Materials, 2023, 35(43): 2206625.

[6] Aurbach D, Markevich E, Salitra G. High Energy Density Rechargeable Batteries Based on Li Metal Anodes. The Role of Unique Surface Chemistry Developed in Solutions Containing Fluorinated Organic Co-solvents[J]. Journal of the American Chemical Society, 2021, 143(50): 21161-21176.

[7] Chen Y L, Yu Z, Rudnicki P, et al. Steric Effect Tuned Ion Solvation Enabling Stable Cycling of High-Voltage Lithium Metal Battery[J]. Journal of the American Chemical Society, 2021, 143(44): 18703-18713.

[8] Dong T T, Zhang S H, Ren Z Q, et al. Electrolyte Engineering Toward High Performance High Nickel (Ni≥80%) Lithium-Ion Batteries[J]. Advanced Science, 2024, 11(7): 2305753.

[9] Lu G X, Nai J, Luan D Y, et al. Surface engineering toward stable lithium metal anodes[J]. Science Advances, 2023, 9(14): eadf1550.

[10] Dong Q Y, Wu J H, Wang Y Q, et al. Bifunctional self-assembled molecular layer enables stable Ni-rich cathodes[J]. Energy Storage Materials, 2023, 63:103054.

[11] Adenusi H, Chass G A, Passerini S, et al. Lithium Batteries and the Solid Electrolyte Interphase (SEI)-Progress and Outlook[J]. Advanced Energy Materials, 2023, 13(10): 2203307.

[12] Cheng H R, Sun Q J, Li L L, et al. Emerging Era of Electrolyte Solvation Structure and Interfacial Model in Batteries[J]. Acs Energy Letters, 2022, 7(1): 490-513.

[13] Tan J, Matz J, Dong P, et al. A Growing Appreciation for the Role of LiF in the Solid Electrolyte Interphase[J]. Advanced Energy Materials, 2021, 11(16): 2100046.

[14] Piao Z H, Xiao P T, Luo R P, et al. Constructing a Stable Interface Layer by Tailoring Solvation Chemistry in Carbonate Electrolytes for High-Performance Lithium-Metal Batteries[J]. Advanced Materials, 2022, 34(8): 2108400.

[15] Li Y, Wu F, Li Y, et al. Ether-based electrolytes for sodium ion batteries[J]. Chemical Society Reviews, 2022, 51(11): 4484-4536.

[16] Wang Z J, Che X L, Wang D N, et al. Non-Fluorinated Ethers to Mitigate Electrode Surface Reactivity in High-Voltage NCM811-Li Batteries[J]. Angewandte Chemie-International Edition, 2024, 63(25): e202404109.

[17] Wang S Z, Shi J Y, Liu Z H, et al. Advanced Ether-Based Electrolytes for Lithium-ion Batteries[J]. Advanced Energy Materials, 2024,14(37): 2401526.

[18] Tian Y F, Tan S J, Lu Z Y, et al. Insights into Anion-Solvent Interactions to Boost Stable Operation of Ether-Based Electrolytes in Pure-SiOx||$LiNi_{0.8}Mn_{0.1}Co_{0.1}O_2$ Full Cells[J]. Angewandte Chemie-International Edition, 2023, 62(33): e202305988.

[19] Peng X D, Wang T S, Liu B, et al. A solvent molecule reconstruction strategy enabling a high-voltage ether-based electrolyte[J]. Energy & Environmental Science, 2022, 15(12): 5350-5361.

[20] Jiang Z P, Yang T, Li C, et al. Synergistic Additives Enabling Stable Cycling of Ether Electrolyte in 4.4 V Ni-Rich/Li Metal Batteries[J]. Advanced Functional Materials, 2023, 33(51): 2306868.

[21] Wang H W, Zhang J K, Zhang H D, et al. Regulating interfacial structure enables high-voltage dilute ether electrolytes[J]. Cell Reports Physical Science, 2022, 3(6): 100919.

[22] Jiang Z P, Deng Y, Mo J S, et al. Switching Reaction Pathway of Medium-Concentration Ether Electrolytes to Achieve 4.5 V Lithium Metal Batteries[J]. Nano Letters, 2023, 23(18): 8481-8489.

[23] Xia D W, Tao L, Hou D, et al. A Green, Fire-Retarding Ether Solvent for Sustainable High-Voltage Li-Ion Batteries at Standard Salt Concentration[J]. Advanced Energy Materials, 2024, 14(38): 2400773.

[24] Yamada Y, Wang J H, Ko S, et al. Advances and issues in developing salt-concentrated battery electrolytes[J]. Nature Energy, 2019, 4(4): 269-280.

[25] Qian J F, Henderson W A, Xu W, et al. High rate and stable cycling of lithium metal anode[J]. Nature Communications, 2015, 6 (1): 6362.

[26] Peng X D, Lin Y K, Wang Y, et al. A lightweight localized high-concentration ether electrolyte for high-voltage Li-Ion and Li-metal batteries[J]. Nano Energy, 2022, 96: 107102.

[27] Li A M, Borodin O, Pollard T P, et al. Methylation enables the use of fluorine-free ether electrolytes in high-voltage lithium metal batteries[J]. Nature Chemistry, 2024, 16(6): 922-929.

[28] Li Z, Rao H, Atwi R, et al. Non-polar ether-based electrolyte solutions for stable high-voltage non-aqueous lithium metal batteries[J]. Nature Communications, 2023, 14(1): 868.

[29] Piao N, Wang J Z, Gao X N, et al. Designing Temperature-Insensitive Solvated Electrolytes for Low-Temperature Lithium Metal Batteries[J]. Journal of the American Chemical Society, 2024,146(27), 18281–18291.

[30] Fang M M, Yue X Y, Dong Y T, et al. A temperature-dependent solvating electrolyte for wide-temperature and fast-charging lithium[J]. Joule, 2024, 8(1): 91-103.

[31] Zhao Q, Stalin S, Archer L A. Stabilizing metal battery anodes through the design of solid electrolyte interphases[J]. Joule, 2021, 5(5): 1119-1142.

[32] Wang J Y, Huang W, Pei A, et al. Improving cyclability of Li metal batteries at elevated temperatures and its origin revealed by cryo-electron microscopy[J]. Nature Energy, 2019, 4(8): 664-670.

[33] Lai P B, Zhang Y Q, Huang B Y, et al. Revealing the evolution of solvation structure in low-temperature electrolytes for lithium batteries[J]. Energy Storage Materials, 2024, 67: 103314.

[34] Wang M L, Yin L M, Zheng M T, et al. Temperature-responsive solvation enabled by dipole-dipole interactions towards wide-temperature sodium-ion batteries[J]. Nature Communications, 2024, 15(1): 8866.

[35] Zhang S Q, Li R H, Deng T, et al. Oscillatory solvation chemistry for a 500 Wh kg^{-1} Li-metal pouch cell[J]. Nature Energy, 2024, 9(10): 1285-1296.

[36] Xiao P T, Yun X R, Chen Y F, et al. Insights into the solvation chemistry in liquid electrolytes for lithium-based rechargeable batteries[J]. Chemical Society Reviews, 2023, 52(15): 5255-5316.

[37] Yang Y S, Wang X F, Zhu J C, et al. Dilute Electrolytes with Fluorine-Free Ether Solvents for 4.5 V Lithium Metal Batteries[J]. Angewandte Chemie-International Edition, 2024, 63(40): e202409193.

[38] Wang Z C, Han R, Zhang H Y, et al. An Intrinsically Nonflammable Electrolyte for Prominent-Safety Lithium Metal Batteries with High Energy Density and Cycling Stability[J]. Advanced Functional Materials, 2023, 33(24): 2215065.

[39] Han S D, Allen J L, Jónsson E, et al. Solvate Structures and Computational/Spectroscopic Characterization of Lithium Difluoro(oxalato)borate (LiDFOB) Electrolytes[J]. Journal of Physical Chemistry C, 2013, 117(11): 5521-5531.

[40] Wang C, Zhao X X, Li D B, et al. Anion-modulated Ion Conductor with Chain Conformational Transformation for stabilizing Interfacial Phase of High-Voltage Lithium Metal Batteries[J]. Angewandte Chemie-International Edition, 2024, 63(19): e202317856.

[41] Wang Z, Zhang H, Xu J, et al. Advanced Ultralow-Concentration Electrolyte for Wide-Temperature and High-Voltage Li-Metal Batteries[J]. Advanced Functional Materials, 2022, 32(23): 2112598.

[42] Wang X S, Wu J R, Zhao Y, et al. Non-solvating fluorosulfonyl carboxylate enables temperature-tolerant lithium metal batteries[J]. Journal of Energy Chemistry, 2023, 82: 287-295.

[43] Thenuwara A C, Shetty P P, Kondekar N, et al. Efficient Low-Temperature Cycling of Lithium Metal Anodes by Tailoring the Solid-Electrolyte Interphase[J]. ACS Energy Letters, 2020, 5(7): 2411-2420.

[44] Park G, Lee K, Yoo D J, et al. Strategy for Stable Interface in Lithium Metal Batteries: Free Solvent Derived vs Anion Derived[J]. ACS Energy Letters, 2022, 7(12): 4274-4281.

[45] Li J Y, Li W D, You Y, et al. Extending the Service Life of High-Ni Layered Oxides by Tuning the Electrode-Electrolyte Interphase[J]. Advanced Energy Materials, 2018, 8(29): 1801957.

[46] Mao M L, Ji X, Wang Q Y, et al. Anion-enrichment interface enables high-voltage anode-free lithium metal batteries[J]. Nature Communications, 2023, 14(1): 1082.

[47] Li J Y, Li W D, Wang S Y, et al. Facilitating the Operation of Lithium-Ion Cells with High-Nickel Layered Oxide Cathodes with a Small Dose of Aluminum[J]. Chemistry of Materials, 2018, 30(9): 3101-3109.